Spatio-temporal dynamics of American plaice (*Hippoglossoides platessoides*) in US waters of the northwest Atlantic

Alexander Hansell[1], Larry Alade[1], Andrew Allyn[2], Lauran Brewster[3], Steve Cadrin[4], Lisa Kerr[2], Others…

1) Northeast Fishery Science Center, NOAA, Woods Hold, MA, USA
2) Gulf of Maine Research Institute, Portland ME, USA
3) Florida Atlantic University, Fort Pierce FL, USA
4) School for Marine Science and Technology, University of Massachusetts Dartmouth, New Bedford, MA, USA.

Abstract:

This work supports the 2022 American plaice (*Hippoglossoides platessoides*) research track stock assessment. Data was compiled from four bi-annual trawl surveys: The Northeast Fisheries Science center (NEFSC) Albatross (1963 – 2008); NEFSC Bigelow (2009– 2019) Maine New Hampshire (MENH; 2005 – 2019); and Massachusetts Division of Marine Fisheries (MADMF; 1981 – 2019). A vector auto-regressive spatio-temporal model (VAST) was applied to the different trawl surveys to estimate changes in spatial distribution and create standardized indices of abundance. Results suggest that the effective area of American plaice has decreased and the center of gravity has been variable. Model selection indicated that bottom temperature and depth were both important modulates of density. Spatio-temporal indices are similar to designed based estimates for the NEFSC and MADMF surveys; however, they are different for the MENH survey. The combined index that incorporates all data is most similar to the NEFSC survey. The results presented here document spatial-temporal changes of American plaice and provide indices that account for these changes, which can be explored within the stock assessment.

Introduction:

Over time, oceanographic conditions have changed in the northwest Atlantic and many species in this area have exhibited changing spatial distributions (Nye et al., 2009; Pinsky et al., 2013). Distribution shifts in the region have been attributed to local environmental variables (SST), regional drivers (e.g., length of summer; Henderson et al. 2017), basin wide climate indices (e.g., AMO; Nye et al., 2009), prey distribution (Golet et al., 2013) and fishing induced changes (Adams et al., 2018).

In the northwest Atlantic, American plaice are hypothesized to be highly sensitivity to climate change and thought to be susceptible to climate-related distribution changes (Hare et al. 2016). Shifting distributions can complicate the interpretation of stock assessments because a shift in the spatial distribution can alter the availability of fish to a specific survey, which can be misinterpreted as a stock decline or increase depending on the direction of the shift (Wilberg et al. 2010, Link et al 2011). The past stock assessment for American plaice removed the Massachusetts Division of Marine Fisheries (MADMF) survey due to diagnostics and the hypothesis that fish have shifted deeper outside of the state survey strata. Despite this hypothesis it is unclear if shifts have occurred and if so, what is driving these shifts.

Spatio-temporal models have the ability to account for spatial shifts and can yield more precise/accurate indices (Shelton et al. 2014). Fitting assessments to these models can also lead to less retrospective bias and outperform assessments with design based indices (Cao et al. 2017). For the 2022 American plaice research track assessment, we fit a vector auto-regressive spatio-temporal model (VAST) to explore distribution shifts of American plaice and create indices of abundance. This work directly helps to address Term of Reference one (ToR; “Identify relevant ecosystem and climate influences on the stock”) and ToR 3 (“Describe the spatial and temporal distribution of the [survey] data. Characterize the uncertainty in these sources of data”).

Methods:

Data:

Data was compiled from four bi-annual trawl surveys: The Northeast Fisheries Science Center (NEFSC) Albatross (1963 – 2008) and Bigelow (2009 – 2019); Maine New Hampshire (MENH; 2005 – 2019); and Massachusetts Division of Marine Fisheries (MADMF; 1981 – 2019; Figure 1). Following recommendations from the American Plaice Research Track Stock Assessment Working Group only strata used in previous assessments were explored for the MADMF survey, while for the NEFSC survey the same strata were used

with the inclusion of three inshore strata (Figure 1). Data collected from the surveys and used in model development are: catch (kg), latitude, longitude, bottom temperature and depth.

Model:

VAST is a delta-model that models the probability of an encounter and positive catch rate as two separate generalized linear mixed models. Here we use a Bernoulli distribution for probability of a positive catch and a gamma distribution for positive catch.

$$logit(p_i) = \gamma_p(t_i c_i) + \omega_p(s_i c_i) + \epsilon_p\left(s_i, c_i, t_i\right) + \sum_{j=1}^{n_j} \alpha_p(j, c_i) x(j, s_i t_i) + \sum_{k=1}^{n_k} \gamma_p(k) q(k, s_i t_i)$$

$$log(\lambda_i) = \gamma_\lambda(t_i c_i) + \omega_\lambda(s_i c_i) + \epsilon_\lambda\left(s_i, c_i, t_i\right) + \sum_{j=1}^{n_j} \alpha_\lambda(j, c_i) x(j, s_i t_i) + \sum_{k=1}^{n_k} \gamma_\lambda(k) q(k, s_i t_i)$$

Where $\gamma_p(t_i c_i)$ is the intercept of the probability of occurrence for year t and length-group c and is modeled as a random walk, $\omega_p(s_i c_i)$ is a time-invariant unexplained spatial effect for knot s and length-group c, and $\epsilon_p\left(s_i, c_i, t_i\right)$ is a time-varying unexplained spatial effect for knot s and length-group c in year t (i.e., an interaction of spatial variation and year). $\alpha_p(j, c_i)$ is the effect of covariate j on length-group c and $x(j, s_i t_i)$ is the value of covariate j in knot s in year t. $\gamma_p(k)$ is a calibration effect converting state survey units to NMFS units (i.e., a statistical vessel calibration), and $q(k, s_i t_i)$ is an indicator variable for state survey units. Both p_i and λ_i must be positive, and p_i must be bounded within [0,1]. Therefore a logit-link is used for p_i and a log-link is used for λ_i. Parameters are defined identically for the expected biomass given occurrence model of $\log(\lambda_i)$.

The spatial processes $\omega_p(s_i c_i)$ and $\omega_\lambda(s_i c_i)$ are modeled as Gaussian Markov random fields with correlations over two spatial dimensions and among length bins.

$$vec(\Omega_\lambda) \sim GRF(0, R_\lambda \otimes V_{\omega\lambda})$$

where Ω_λ is a matrix composed of $\omega_\lambda(s, c)$ at every knot s and length bin c, R_λ is the correlation among knots, and $V_{\omega\lambda}$ is the correlation among length bins

$$L_{\omega\lambda} = L_{\omega\lambda} L_{\omega\lambda}^{T}$$

where $L_{\omega\lambda}$ is a loadings matrix representing covariance among length bins. Spatial covariance between knots s and s* is modeled as a Matern process.

$$R_{\lambda}(s, s^{*}) = \frac{1}{2^{v-1}\Gamma(v)} (k_{\lambda}\mathrm{H}|s - s^{*}|)^{v} K_{v}(k_{\lambda}\mathrm{H}|s - s^{*}|)$$

Where v is a smoothness parameter that is fixed at 1.0, k_{λ} controls the distance over which correlation declines to zero, is a Bessel function, and H is a two-dimensional anisotropic distance function. The spatio-temporal processes $\varepsilon_{p}(s_i, c_i, t_i)$and $\varepsilon_{\lambda}(s_i, c_i, t_i)$ are fit independently to each year and are also modeled as Gaussian Markov random fields with Matern covariance.

Derived quantities:

The expected biomass in a knot is the expected density in that knot multiplied by the area associated with that knot.

$$\hat{B}_{s,c,t} = a(s) x logit^{-1}(\lambda_{p}(t, c) + (\omega_{p}(s, c) + \epsilon_{p}(s, c, t) + \sum_{j=1}^{n_j} \alpha_{p}(j, c) x(j, s, t)) \; x \; \exp(\Upsilon_{\lambda}(t, c) + (\omega_{\lambda}(s, c) + \epsilon_{\lambda}(s, c, t) + \sum_{k=1}^{n_k} \alpha_{\lambda}(j, c) x(j, s, t))$$

where a(s) is the area of knot s and $\hat{B}_{s,c,t}$is the expected biomass in knot s for size-category c in year t. The total biomass of size-category c in year t is then

$$\hat{B}_{s,c,t} = \sum_{s=1}^{n_s} \hat{B}_{s,c,t}$$

where n_s is the number of knots.

Covariates:

A factor was used to account for vessel effects between the four different surveys. Local covariates vary across space, while regional covariates are univariate and represent temporal changes across the entire stock. For local covariates, we explored bottom temperature and depth associated with each tow (Figure 2). For regional covariates, we explored the AMO and NAO (Figure 3).

In VAST, the spatial random fields account for the changes in distribution throughout time and capture residual patterns that cannot be attributed to fixed effects (explanatory covariates). Thus, we can determine the importance of each variable in potential distribution shifts by setting the spatial effects of the model to zero and generating a time series of center-of-gravity estimates. The center-of-gravity estimates from the model without the random fields are then compared to the model with random fields to determine the amount of variation caused by each covariate; this process is referred to as counterfactual analysis (Pearl, 2009; Perretti and Thorson, 2019). Collinearity of covariates was examined using generalized variance-inflation factor (GVIF) scores. Any covariate with a score greater than three was removed, and the GVIFs were recalculated (Zuur, et al. 2012). For index standardization, Akaike Information Criterion (AIC) scores were used to determine the best-fitting model. If AIC scores were within two units of one another, the most parsimonious model was selected (Burnham and Anderson, 2004).

Results:

Models failed to converge when either the AMO or NAO was included. Models with local covariates converged and diagnostics did not reveal any major issues. The optimal number of knots was determined to be 200. AIC and model diagnostics suggest that bottom temperature and depth should be included as modulates of density (Table 1).

Over the time series, the center of gravity has been variable in both the spring and fall with periods of northeast and southwest movement. In the spring, on average the American plaice center of gravity has shifted south at 0.1 (SD = 9.9) km/year. In contrast, in the fall on average the American plaice center of gravity has shifted north at 0.3 (SD=7.9) km/year. Average east west shifts were negligible for both seasons (Figure 4). Since the 1960's, the effective area occupied has decreased in the spring and fall by an average rate of 177.9 (SD =9240.4) and 80.6 (SD = 7608.8) km/year (Figure 5). Counterfactual analyses predict that depth is the primary driver of both spring and fall distribution changes (Figure 6 & 7).

The combined spatio-temporal index of abundance is most similar to the NEFSC bottom trawl surveys. VAST estimates of relative abundance for the NEFSC and MADMF trawl surveys are similar to design based estimates. VAST estimates vary compared to design based estimates for the MENH survey, with periods of higher and lower estimates of relative abundance (Figure 8).

Discussion:

The VAST model provides a single spatio-temporal framework to estimate both distribution changes and indices of abundance. VAST selected that bottom temperature and depth are important drivers of density, which agrees with previous studies that have linked both of these covariates to spatial distribution and abundance (Walsh et al. 2004; Robertson et al. 2021). Spatio-temporal models also estimate that distribution shifts have occurred and the effective area occupied by American plaice has decreased (Figure 3 and 4). Similar results for American plaice were observed on the Grand Bank where it was estimated that fish shifted southward and had a range contraction (Robertson et al. 2021).

Spatio-temporal indices of abundance estimate similar trends as design based estimates and the combined index is most similar to the NEFSC survey (Figure 5). Similarities between the NEFSC and the combined index make sense given that VAST uses an area based approach to estimate relative abundance and the spatial footprint of the NEFSC survey is larger than the state surveys. The spatio-temporal indices produced by VAST have a strong track history of being used in stock assessment and for plaice incorporating them could help to account for residual patterns in past stock assessments (Thorson et al. 2015).

Acknowledgments:

We would like to thank the American Plaice Research Track Stock Assessment Working Group for their feedback on model development. The scientific results and conclusions, as well as any views or opinions expressed herein, are those of the authors and do not necessarily reflect those of their institutions.

References:

Adams, C.F., Alade, L.A., Legault, C.M., O'Brien, L., Palmer, M.C., Sosebee, K.A., Traver, M.L., 259 2018. Relative importance of population size, fishing pressure and temperature 260 on the spatial distribution

of nine Northwest Atlantic groundfish stocks. PLOS 261 ONE 13, e0196583.
https://doi.org/10.1371/journal.pone.0196583

Burnham, K. P., & Anderson, D. R. (2004). Multimodel inference: understanding AIC and BIC in model selection. *Sociological methods & research*, *33*(2), 261-304.

Cao, J., Thorson, J. T., Richards, R. A., & Chen, Y. (2017). Spatiotemporal index standardization improves the stock assessment of northern shrimp in the Gulf of Maine. *Canadian Journal of Fisheries and Aquatic Sciences*, *74*(11), 1781-1793.

Golet, W.J., Galuardi, B., Cooper, A.B., and Lutcavage, M.E. 2013. Changes in the distribution of Atlantic bluefin tuna (*Thunnus thynnus*) in the Gulf of Maine 1979-2005. PLoS ONE 8(9): e75480. doi:10.1371/journal.pone.0075480

Hare JA, Morrison WE, Nelson MW, Stachura MM, Teeters EJ, Griffis RB, Alexander MA, Scott JD, Alade L, Bell RJ, et al. 2016. A Vulnerability Assessment of Fish and Invertebrates to Climate Change on the Northeast U.S. Continental Shelf. PLOS ONE. 11(2):e0146756.

Henderson, M.E., Mills, K.E., Thomas, A.C., Pershing, A.J., Nye, J.A., 2017. Effects of spring 287 onset and summer duration on fish species distribution and biomass along the 288 Northeast United States continental shelf. Rev. Fish Biol. Fish. 27, 411–424. 289 https://doi.org/10.1007/s11160-017-9487-9

Link, J.S., Nye, J.A., Hare, J.A. 2011. Guidelines for incorporating fish distribution shifts into a fisheries management context. Fish Fish. 12:461-469.

Miller, T. J., Das, C., Politis, P. J., Miller, A. S., Lucey, S. M., Legault, C. M., ... & Rago, P. J. (2010). Estimation of Albatross IV to Henry B. Bigelow calibration factors.

Nye, J. A., Link, J. S., Hare, J. A., & Overholtz, W. J. (2009). Changing spatial distribution of fish stocks in relation to climate and population size on the Northeast United States continental shelf. *Marine Ecology Progress Series*, *393*, 111-129.

Pearl, J. (2009). Causal inference in statistics: An overview. *Statistics surveys*, *3*, 96-146.

Perretti, C. T., & Thorson, J. T. (2019). Spatio-temporal dynamics of summer flounder (Paralichthys dentatus) on the Northeast US shelf. *Fisheries Research*, *215*, 62-68.

Pinsky, M. L., Worm, B., Fogarty, M. J., Sarmiento, J. L., & Levin, S. A. (2013). Marine taxa track local climate velocities. *Science*, *341*(6151), 1239-1242.

Robertson, M. D., Gao, J., Regular, P. M., Morgan, M. J., & Zhang, F. (2021). Lagged recovery of fish spatial distributions following a cold-water perturbation. *Scientific reports*, *11*(1), 1-11.

Shelton, A. O., Thorson, J. T., Ward, E. J., & Feist, B. E. (2014). Spatial semiparametric models improve estimates of species abundance and distribution. *Canadian Journal of Fisheries and Aquatic Sciences*, *71*(11), 1655-1666.

194 Walsh, S. J., Simpson, M., & Morgan, M. J. 2004. Continental shelf nurseries and recruitment variability in
195 American plaice and yellowtail flounder on the Grand Bank: Insights into stock resiliency. *Journal of Sea*
196 *Research*, *51*(3), 271–286.

197 Wilberg, M.J., Thorson, J.T., Linton, B.C., Berkson, J. 2010. Incorporating time-varying catchability into
198 population dynamic stock assessment models. Rev. Fish. Sci. 18: 7-24.

199 Zuur, A.F., Saveliev, A.A., Ieno, E.N., 2012. Zero Inflated Models and Generalized Linear Mixed Models
200 with R. Highland Statistics Ltd, Newburgh

201

Tables:

Table 1: AIC scores for different models looking at environmental variables.

Model	Spring	Fall
Null	AIC	
	387568	425728
+ Depth	386233	424453
+ Depth + Bottom Temp	385716	424232

206 **Figures:**

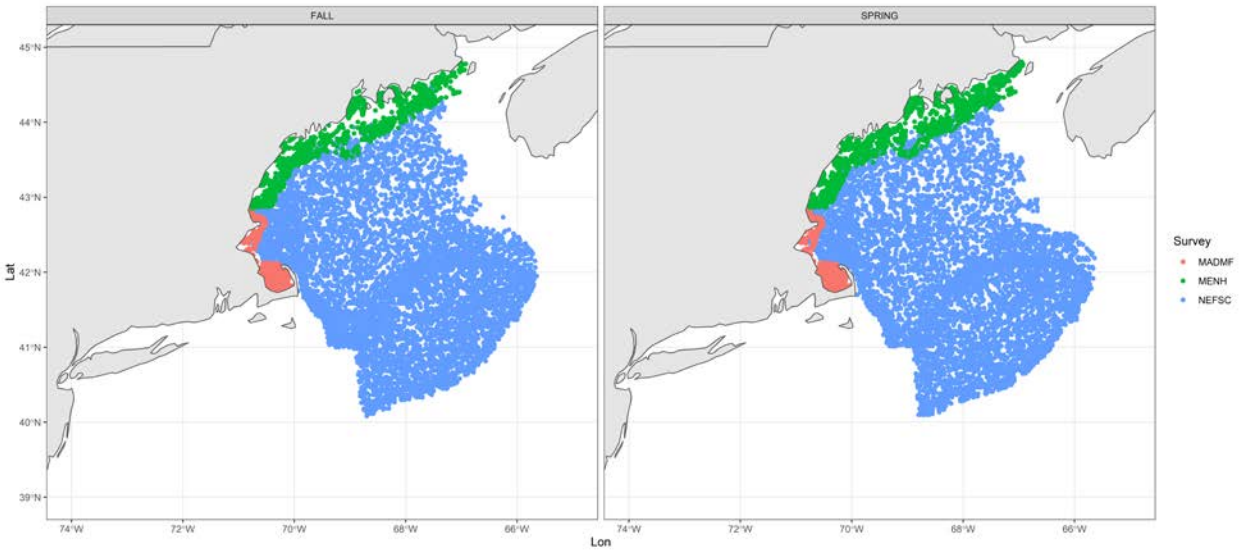

207

208 Figure 1. Map of the different tow locations used in VAST model for American plaice. NEFSC – includes
209 both the Albatross and Bigelow surveys.

210

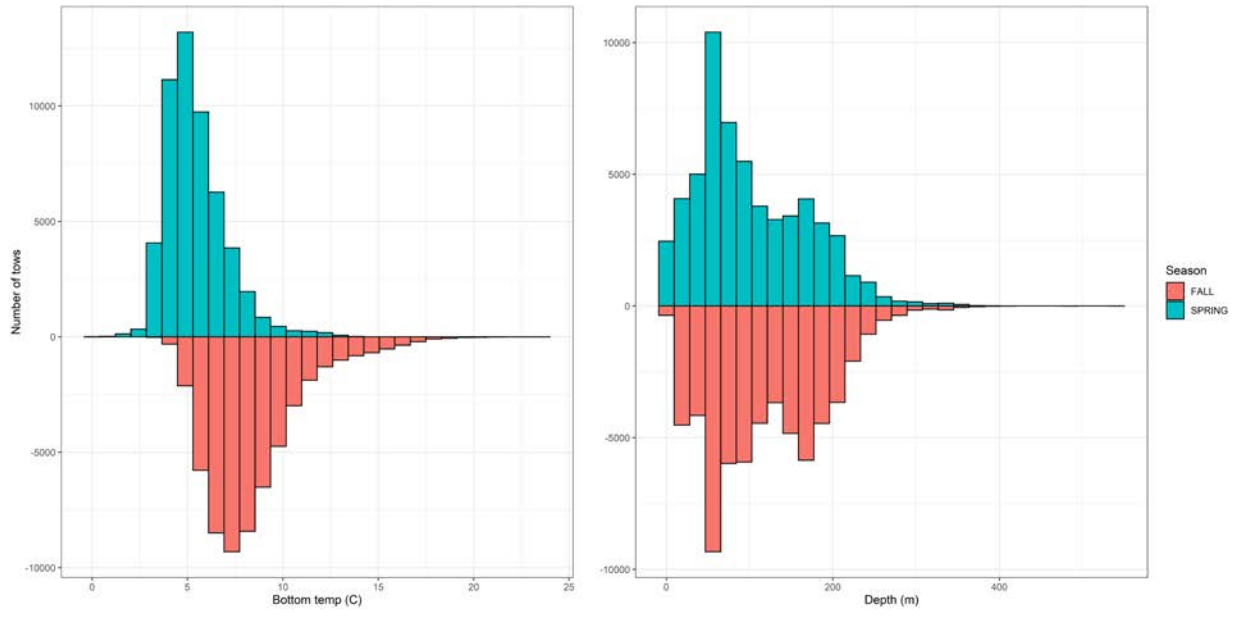

211

212 Figure 2: Distribution of bottom temperature and depth associated with each survey tow.

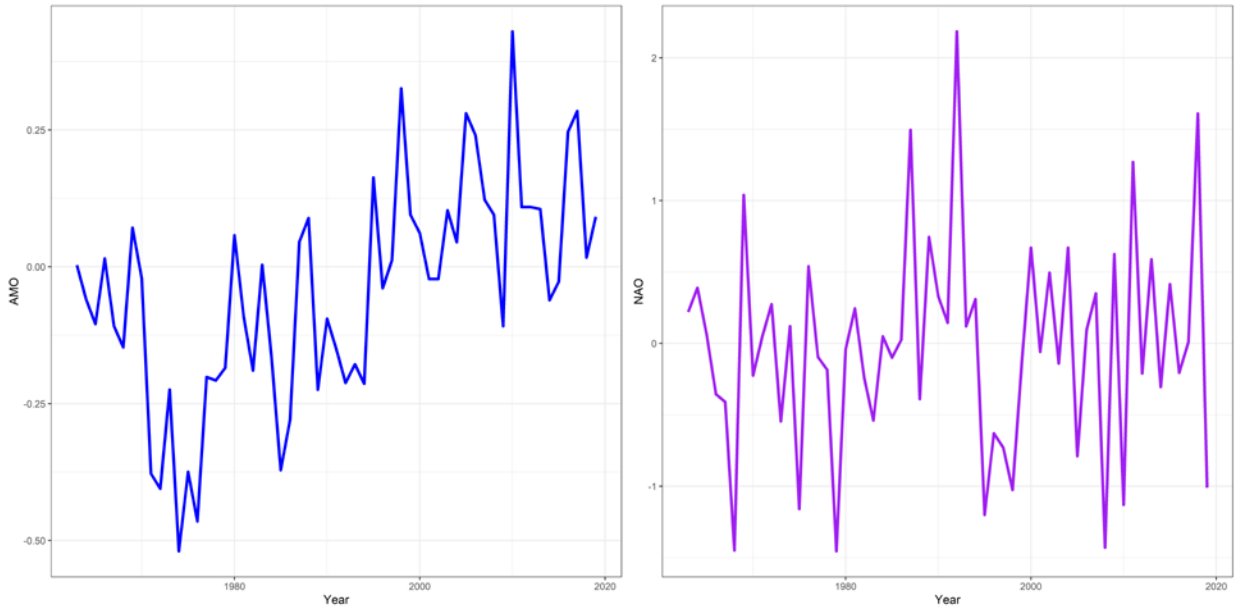

213

214 Figure 3: Regional time series explored in VAST for American plaice.

215

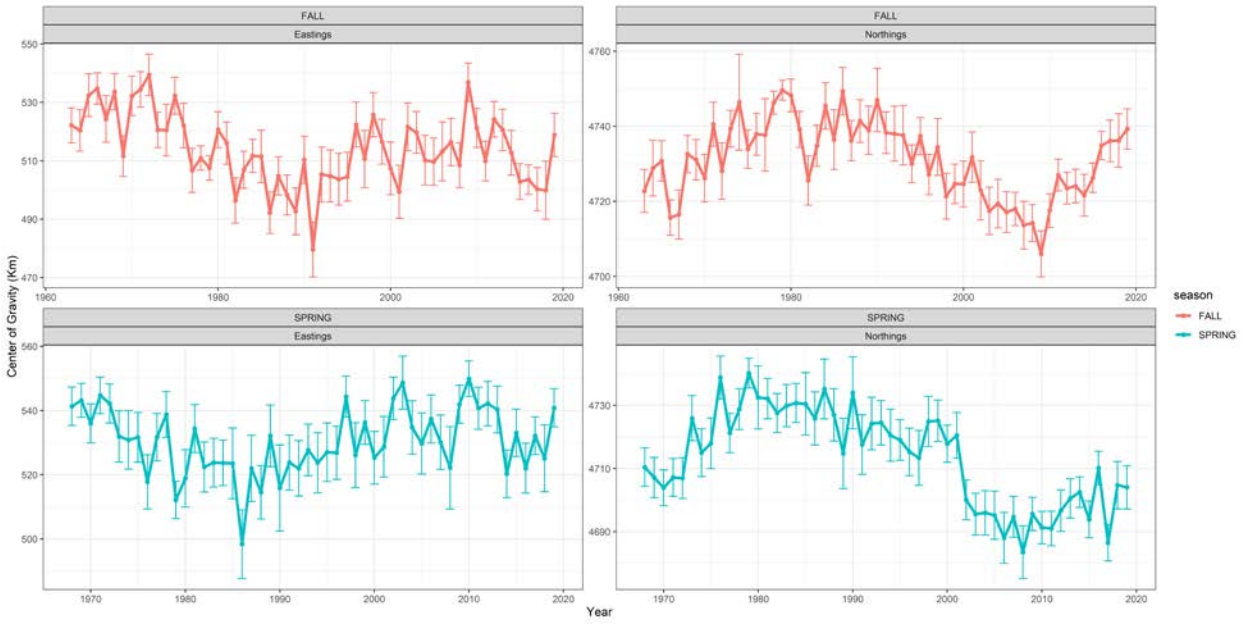

216

217 Figure 4: Center of gravity estimates produced by VAST for American plaice.

218

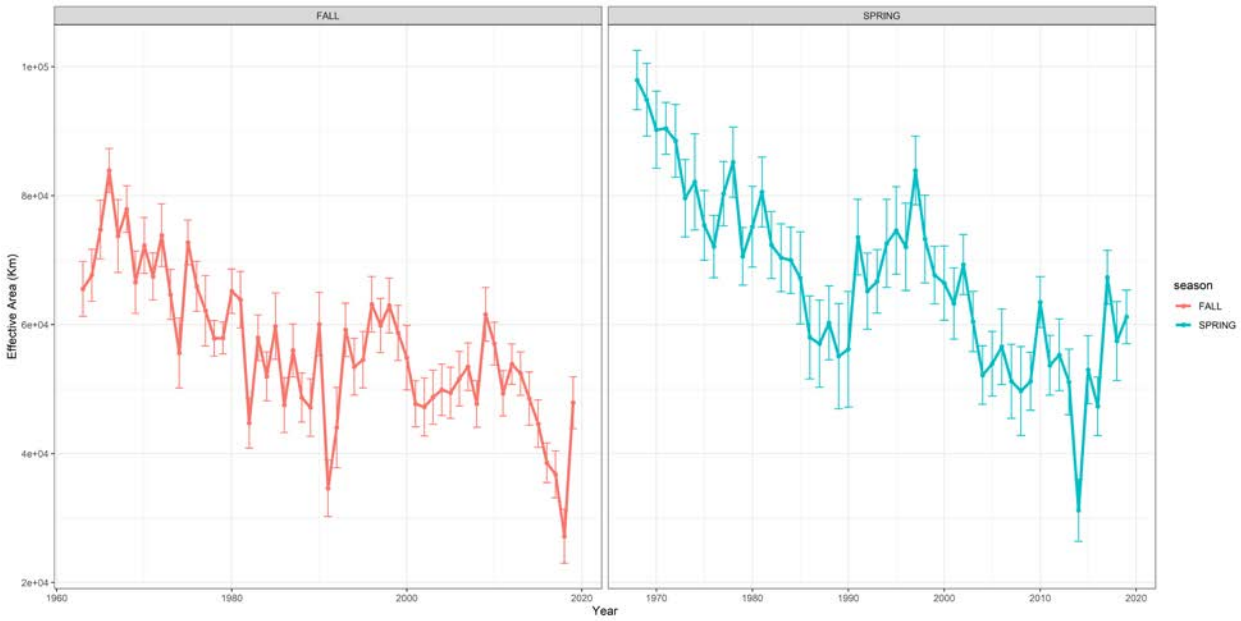

219

220 Figure 5: Effective area estimates produced by VAST for American plaice.

221

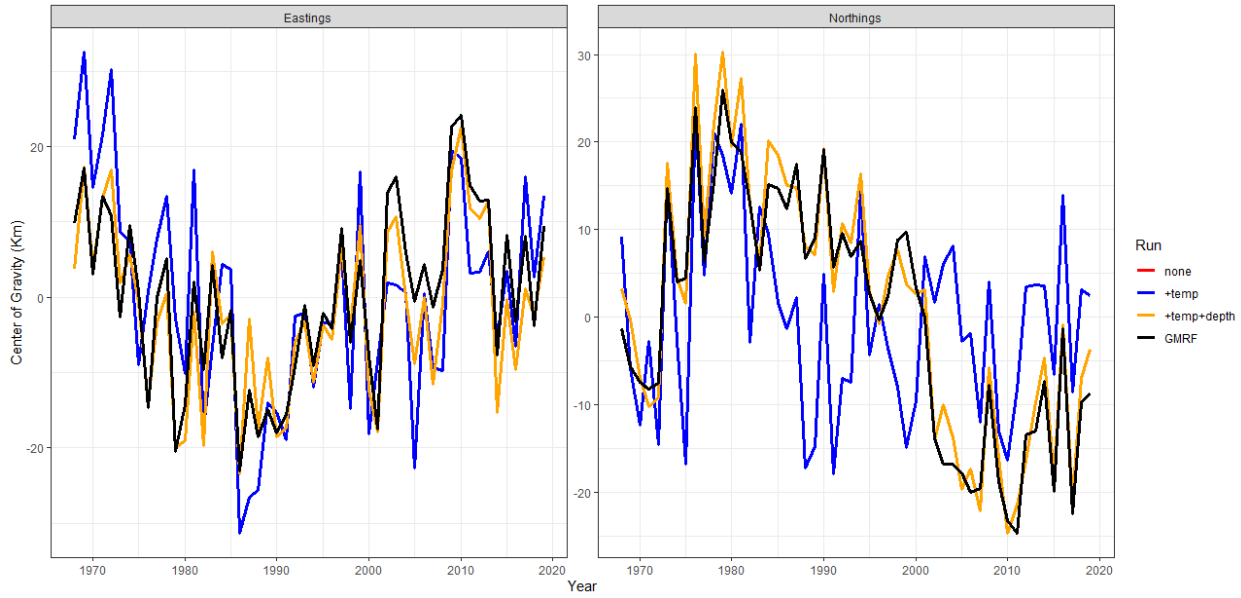

222

223 Figure 6: Counterfactual analysis for spring.

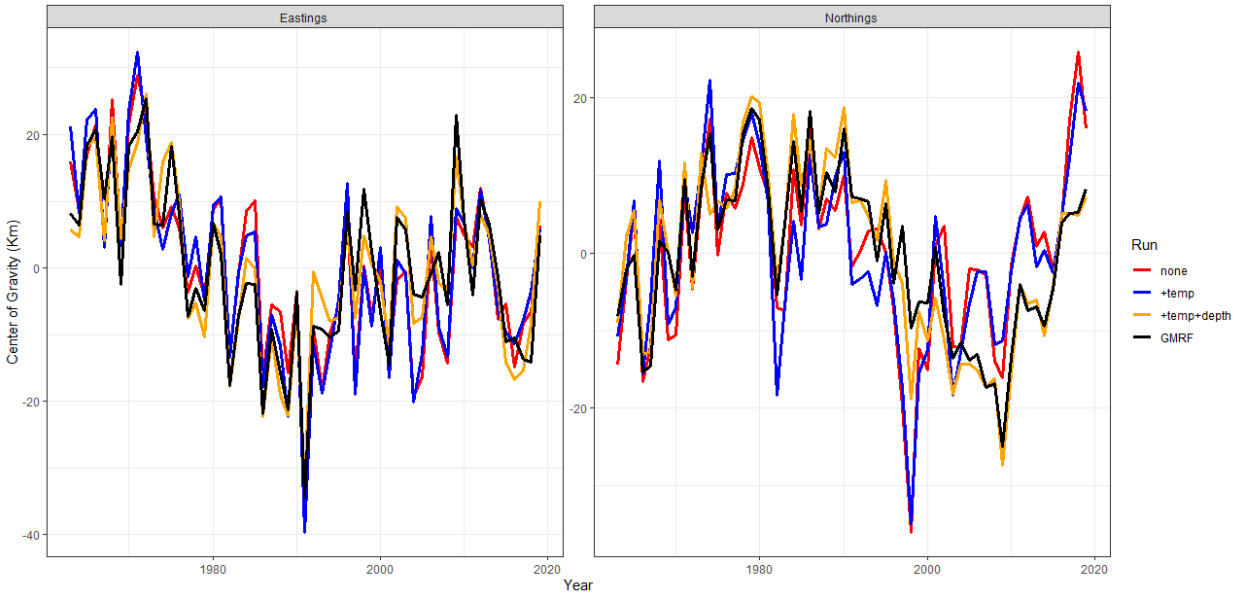

224

225 Figure 7: Counterfactual analysis for fall.

226

227

228 Figure 8: Comparison of designed and VAST estimated indices for the different surveys. “All” is the

229 combined index, which includes all of the surveys.

230

231 Supplemental Material:

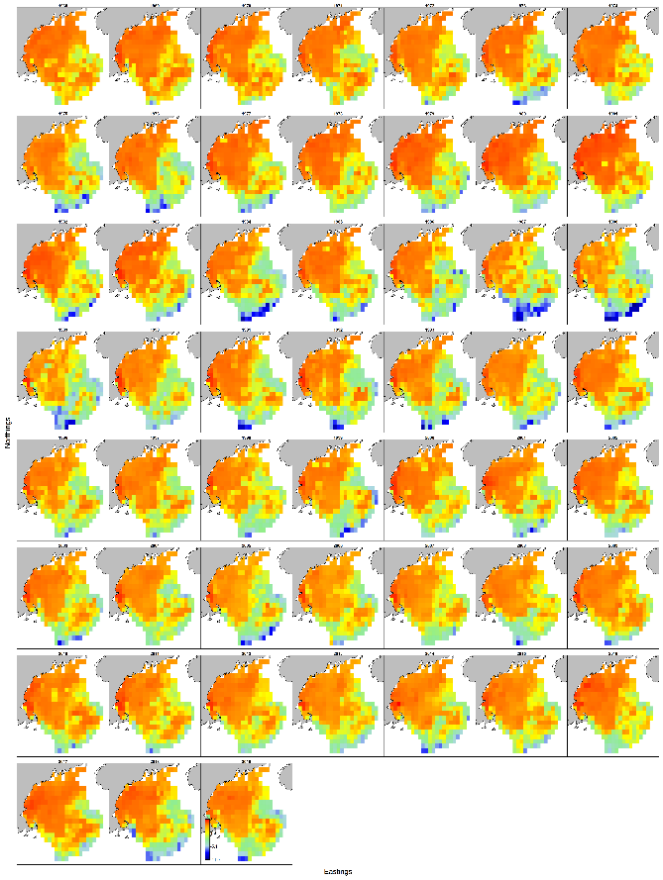

232

233 Figure 1: VAST estimated density in the spring.

234

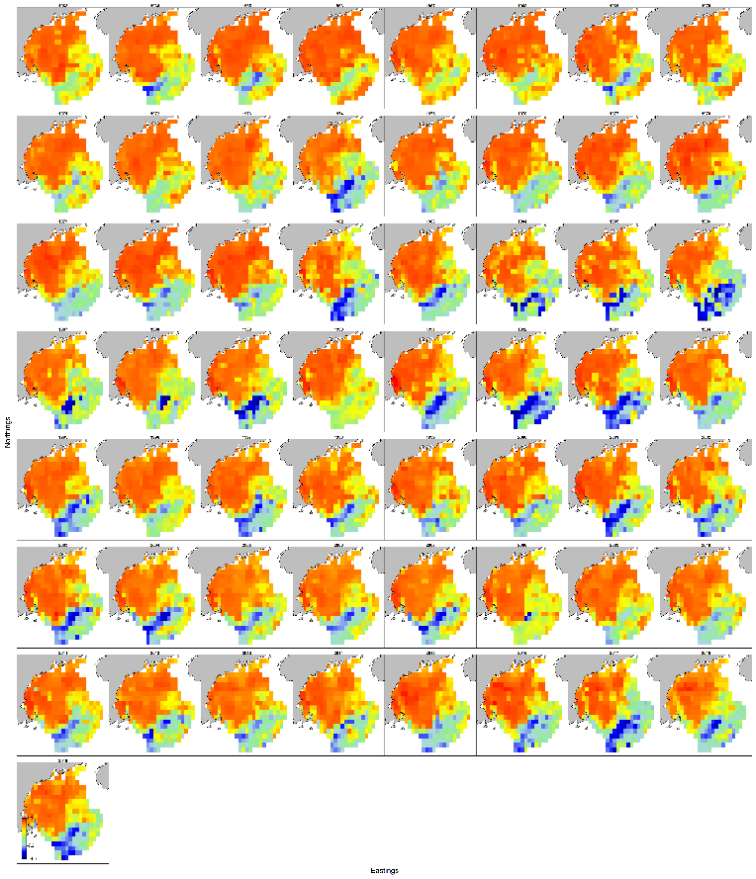

235

236 Figure 2: VAST estimated density in the spring.

237

238

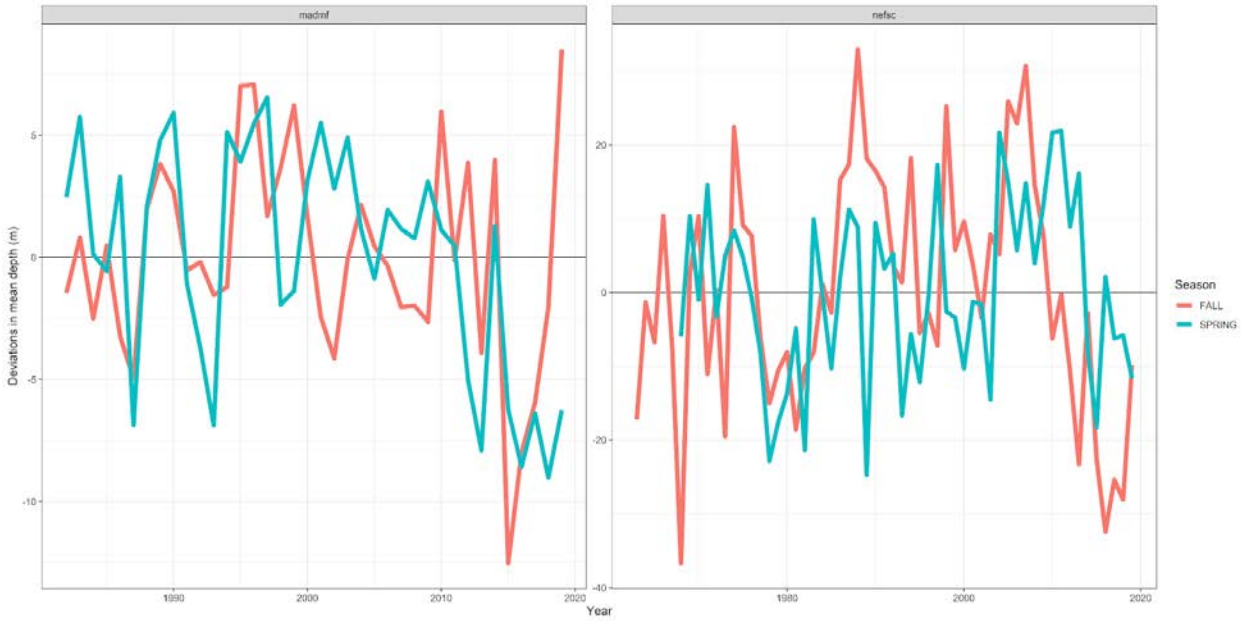

Figure 3: Deviations in depth for MADMF and NEFSC surveys. Negative values are deeper.

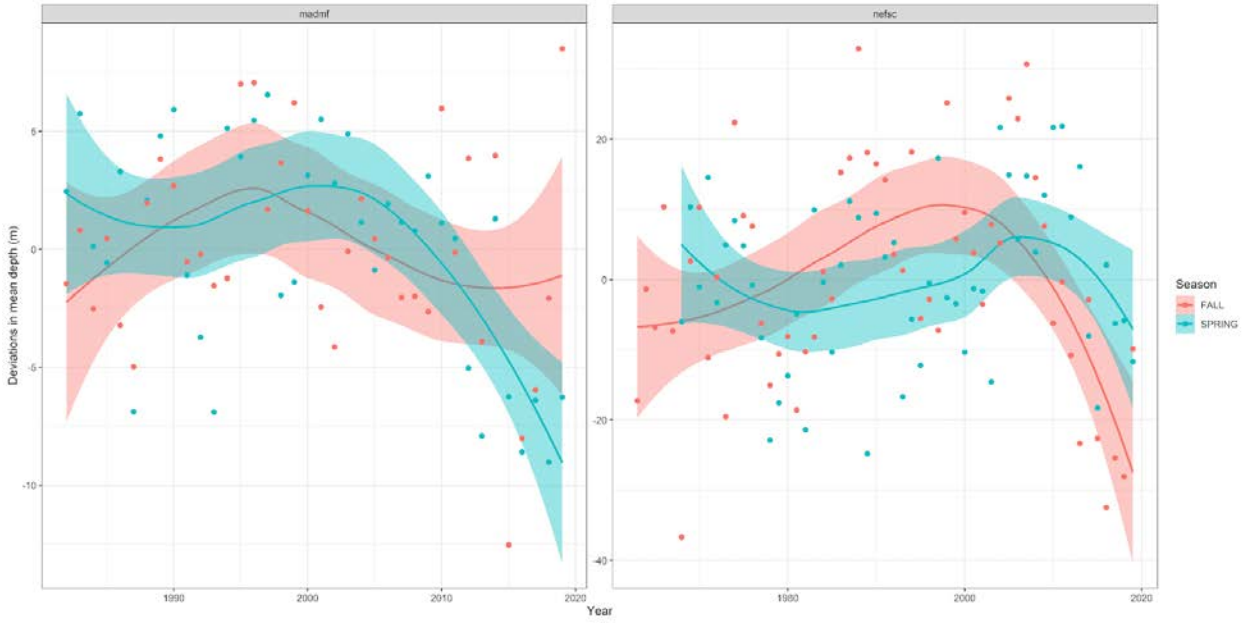

Figure 4: Deviations in depth for MADMF and NEFSC surveys. Fit is a loess smooth and negative values are deeper.

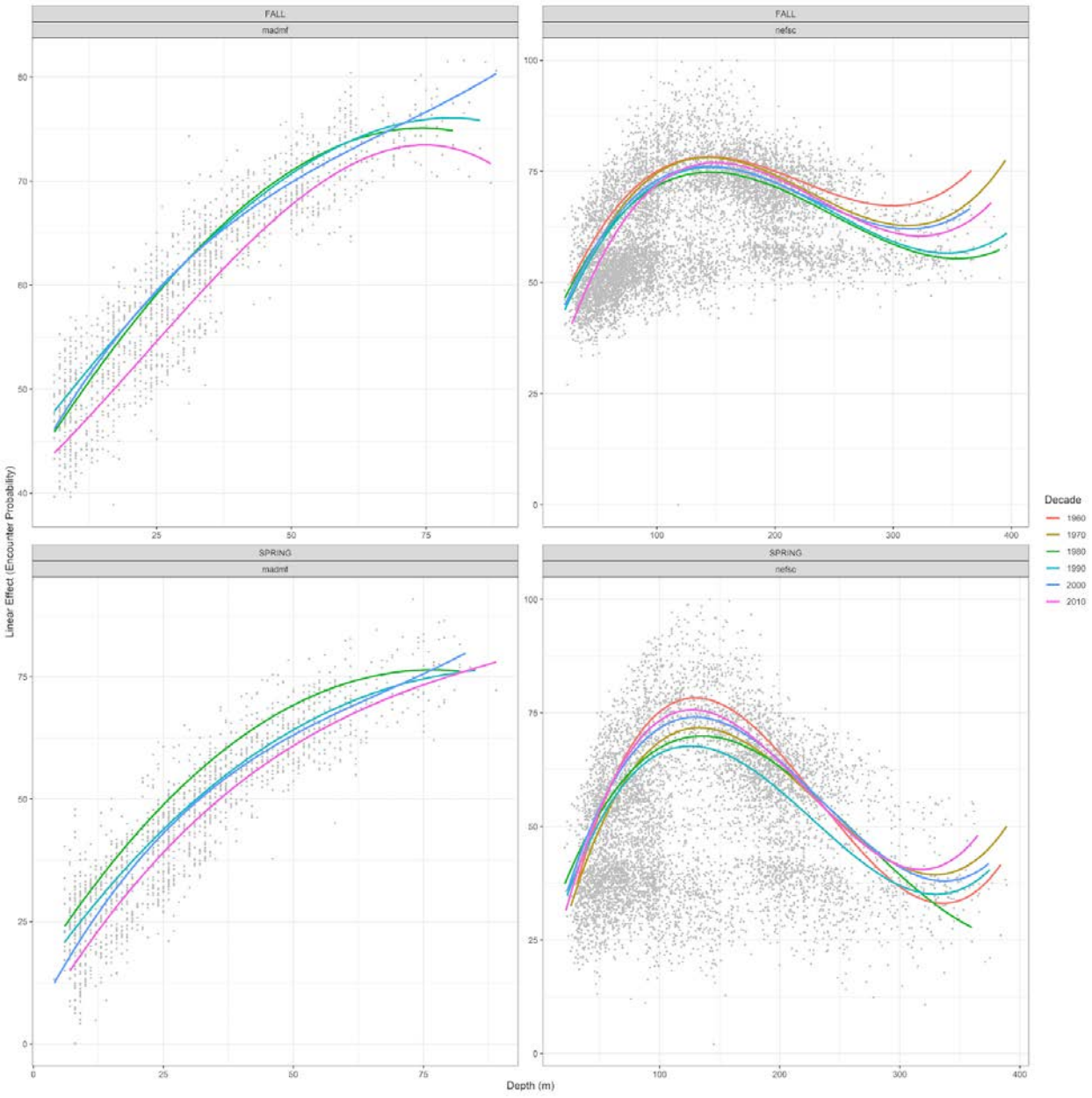

246

247 Figure 5: Encounter probability for plaice by decade, season and survey.

248

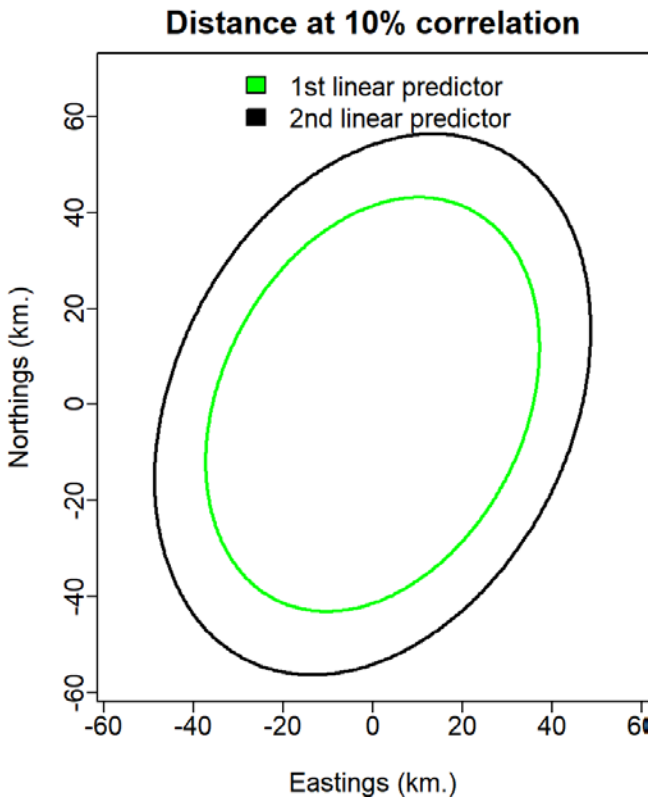

Figure 6: Aniso correlation plot for VAST model investigating spatio-temporal dynamics of American plaice in the spring.

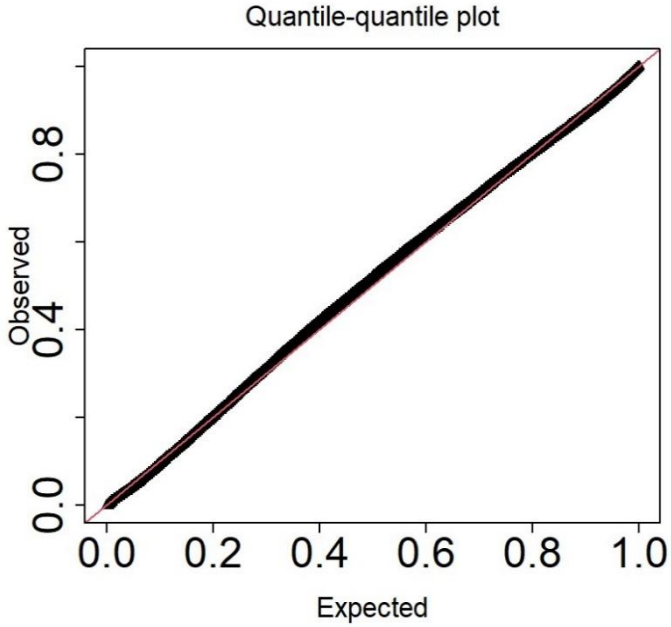

Figure 7: QQ plot for VAST model investigating spatio-temporal dynamics of American plaice in the spring.

255

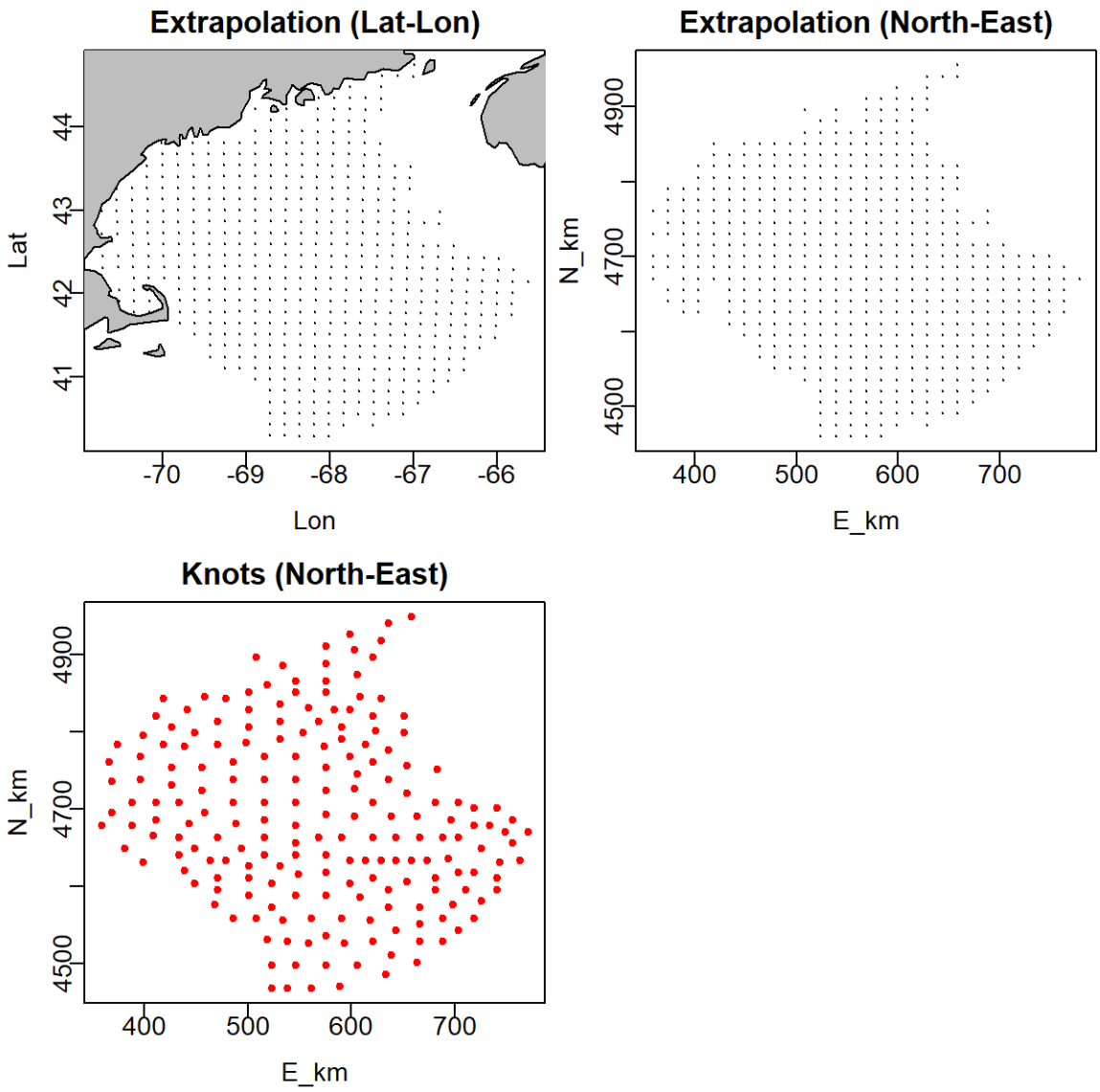

256

257 Figure 8: Knots for VAST model investigating spatio-temporal dynamics of American plaice in the spring
258 and fall.

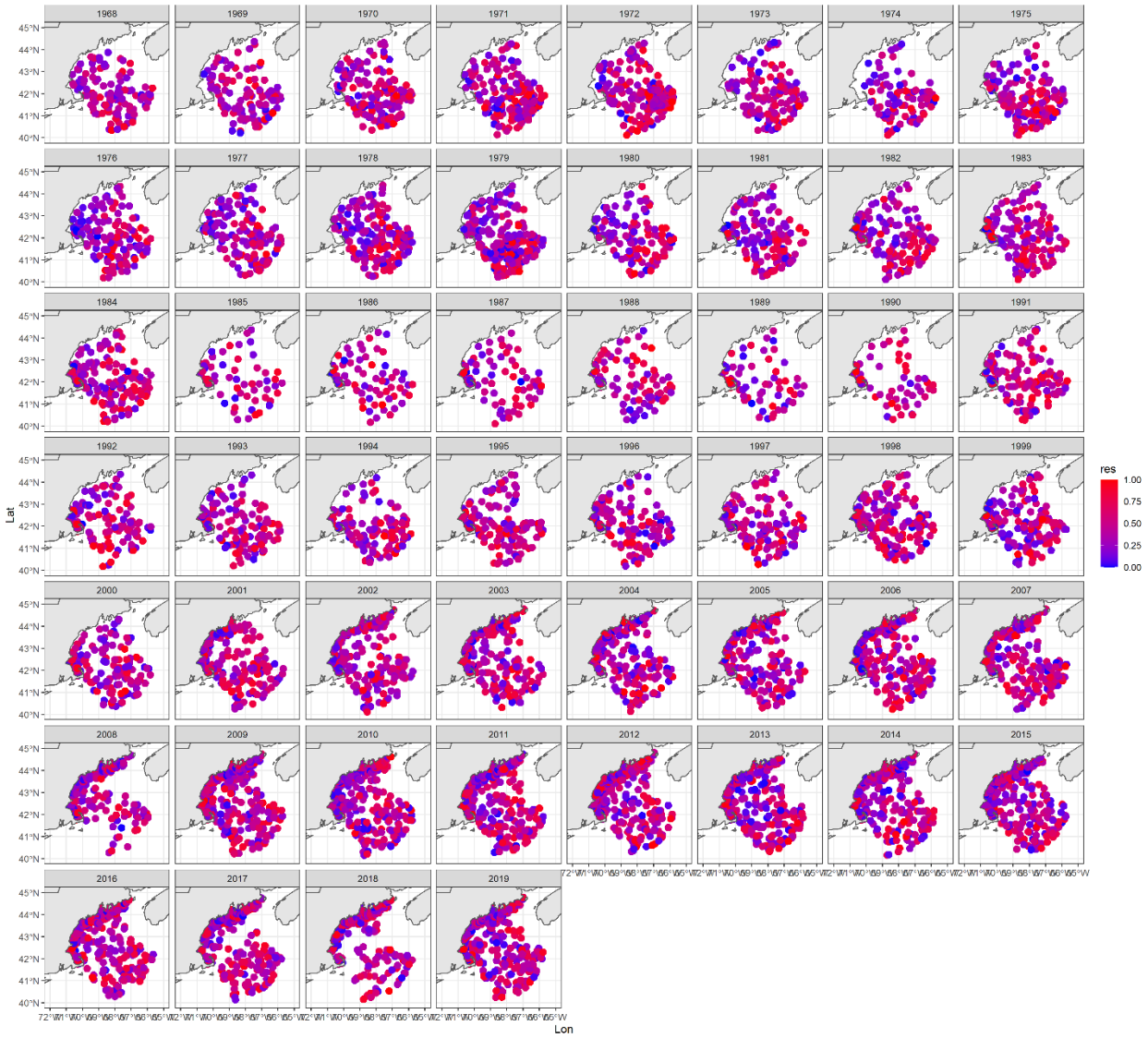

259

260 Figure 9: Spatial residuals for VAST model investigating spatio-temporal dynamics of American plaice in
261 the spring.

262

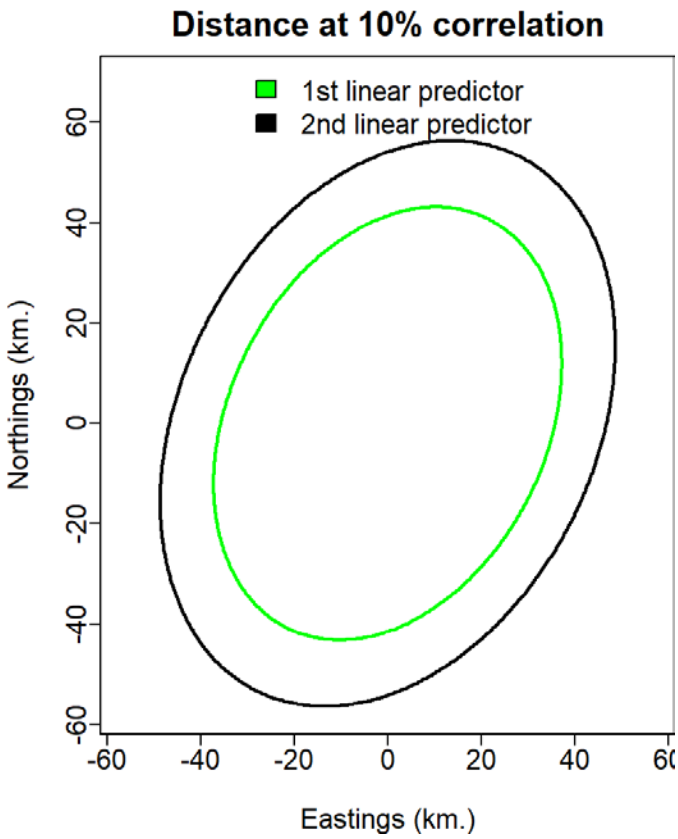

Figure 10: Aniso correlation plot for VAST model investigating spatio-temporal dynamics of American plaice in the fall.

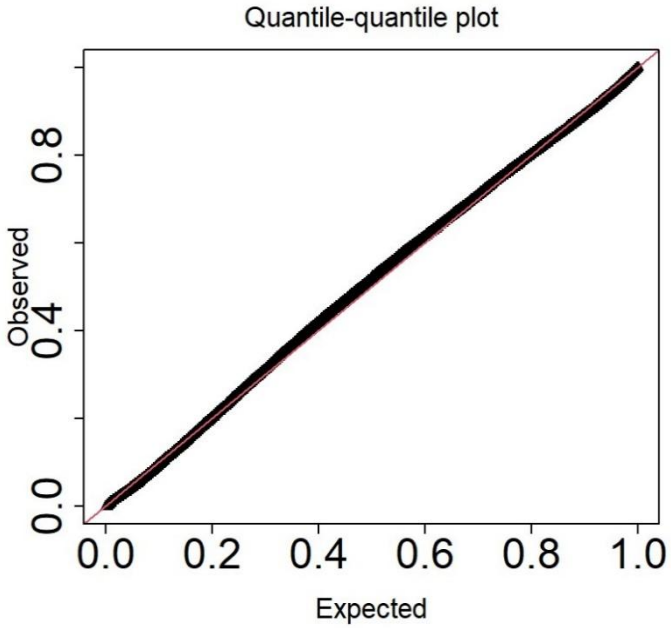

Figure 11: QQ plot for VAST model investigating spatio-temporal dynamics of American plaice in the fall.

268

269

270 Figure 12: Spatial residuals for VAST model investigating spatio-temporal dynamics of American plaice in
271 the fall.